High performance of 3D silicon nanowires array@CrN for electrochemical capacitors

Abdelouadoud Guerra, Emile Haye, Amine Achour, Maxime Harnois, Toufik Hadjersi, Jean-Francois Colomer, Jean-Jacques Pireaux, Stéphane Lucas, Rabah Boukherroub

High performance of 3D silicon nanowires array@CrN for electrochemical capacitors

Abdelouadoud GUERRA[1, 2, 3*], Emile HAYE[4*,*], Amine ACHOUR[4], Maxime HARNOIS[5], Toufik HADJERSI[3], Jean-François COLOMER[6], Jean-Jacques PIREAUX[4], Stéphane LUCAS[7] and Rabah BOUKHERROUB[1]

[1] *Univ. Lille, CNRS, Centrale Lille, ISEN, Univ. Valenciennes, UMR 8520, IEMN, F-59000 Lille, France*

[2] *Université Ferhat Abbas Setif 1, El Bez, Setif 19000, Algeria*

[3] *Centre de Recherche en Technologie des Semi-conducteurs pour L'Energétique (CRTSE), Division TESE, 2 Bd. Frantz Fanon, B.P. 140 Alger-7 Merveilles, Alger, Algeria*

[4] *Laboratoire Interdisciplinaire de Spectroscopie Electronique (LISE), Namur Institute of Structured Matter (NISM), University of Namur, 61 Rue de Bruxelles, 5000 Namur, Belgium*

[5] *Département Microélectronique & Microcapteurs, UMR 6164, Université de Rennes 1 – Campus de Beaulieu, 263 Avenue du Général Leclerc – CS 74205, 35042 Rennes Cedex, France*

[6] *Service de Microscopie électronique, University of Namur, Rue de Bruxelles 61, 5000 Namur, Belgium*

[7] *Laboratoire d'Analyse par Réactions Nucléaires (LARN), Namur Institute of Structured Matter (NISM), University of Namur, 61 Rue de Bruxelles, 5000 Namur, Belgium*

* Corresponding authors: Abdelouadoud Guerra

Email address: guerra_abdelouadoud@yahoo.com - abdelouadoud.guerra.etu@univ-lille.fr

, Corresponding authors: Emile HAYE

Email address: emile.haye@unamur.be

Abstract

Silicon nanowire (SiNWs) arrays were coated with chromium nitride (CrN) for use as super-capacitor electrodes. The CrN layer with different thicknesses were deposited onto SiNWs using bipolar magnetron sputtering method. The areal capacitance of the SiNWs-CrN, as measured in 0.5 M H_2SO_4 electrolyte, was as high as 180 $mF.cm^{-2}$ at a scan rate of 5 $mV.s^{-1}$ (equivalent to 31.8 $mF.cm^{-2}$ at 1.6 $mA.cm^{-2}$) with an excellent electrochemical retention of 92% over 15000 cycles. This work paves the way toward using CrN modified 3D SiNWs arrays for micro-supercapacitor application.

Keywords: Silicon nanowires; Vapor Liquid Solid method; Transition metal nitrides; Chromium nitride; Electrochemical capacitors.

1. Introduction

Electrochemical capacitors (ECs), have attracted increasing attention as potential candidate for energy storage and conversion due to their high power density and long cycling life compared to batteries and electrolytic capacitors [1-4]. Supercapacitors can be classified into two categories: electrochemical double-layer supercapacitors (EDLCs) and pseudo-capacitors [5, 6]. The second category (pseudo-capacitors) which are widely common for transition metal oxides and polymers, offer high specific capacitance, but dotted with moderate cyclic stability and low power density which can be limiting for some applications, where both high power density and long cycling life stability are needed [1].

Recently, silicon nanowires (SiNWs) have been investigated as electrodes in electrochemical capacitors with a special focus on their use as the future on-chip micro-supercapacitors [7-10]. However, the rapid oxidation of silicon surface and the degradation of SiNWs during electrochemical cycling in aqueous electrolytes is the main obstacle for their wide application in the field of ECs and micro-supercapacitors [11, 12]. Nonetheless, this limitation can be overcome by the growth of nanostructures onto the SiNWs surface in order to increase the specific capacitance without scarifying too much the power density and cycling stability of SiNWs. For example, Alper *et al.* [7] have fabricated silicon carbide/SiNWs composites with an enhanced capacitive behavior, and higher capacitance values. Furthermore, carbon/SiNWs have also been reported as composites for ECs with good capacitance and improved cycling life stability [11].

Transition metal nitrides (TMNs) including TiN [13-15], VN [16-18], Mo_2N [19] seem to be a suitable choice due to their high specific capacitance, excellent electrical conductivity and electrochemical stability. Among these TMNs, chromium nitride (CrN) [20, 21] has been recently studied as a promising electrode material for ECs, owing to its excellent conductivity and electrochemical stability [21]. Therefore, coupling the high conductivity of the CrN combined with the large surface area of SiNWs can improve the electrochemical performance and thereby produce enhanced capacitance.

Herein we report the electrochemical investigation of silicon nanowires, coated with CrN layers as electrode materials for ECs. The CrN layers with different thicknesses were grown on SiNWs by magnetron sputtering using one step process. The areal capacitance of SiNWs@CrN was enhanced by 116 fold compared to that of pristine SiNWs in 0.5 M H_2SO_4 electrolyte, with an excellent cycling stability over 15000 cycles. These results demonstrate that coating SiNWs with TMNs such as CrN can push forward toward the use of SiNWs in micro-supercapacitors.

2. Experimental

2.1. Materials and methods

All chemicals and reagents were used without any purification. Acetone, isopropyl, hydrogen peroxide (H_2O_2, 30%), and sulfuric acid (H_2SO_4) were obtained from Sigma-Aldrich.

2.2. Fabrication of silicon nanowires SiNWs on silicon wafer

Single-side polished silicon (100) oriented n-type wafers (0.001-0.005 $Ohm.cm^{-1}$ resistivity) were used as substrate. The substrate was firstly cleaned in acetone and isopropyl to remove organics impurities. Then cleaned in a piranha solution (3:1 H_2SO_4/H_2O_2) at 80 °C followed by rinsing with Milli-Q water and dried under nitrogen.

Silicon nanowires (SiNWs) were prepared using the vapor-liquid-solid (VLS) mechanism [23], based on metal-catalyst-directed chemical vapor deposition. First, a thin film of gold catalyst (4 nm thick) was deposited on the clean Si substrate. Gold colloids are deposited with HF 10% from an aqueous gold colloid solution (BritishBioCell). Then gold thin film is evaporated under UHV on the Si substrate. The gold-coated surface then exposed to silane gas (SiH_4) at a pressure of 0.4 T (Q = 40 sccm) at 500 °C for 60 min for SiNWs growth.

Safety Considerations: The mixture H_2SO_4/H_2O_2 (piranha) solution is a strong oxidant, it can cause severe skin burns.

2.3. Deposition of CrN onto the SiNWs

Chromium nitride (CrN) layers were deposited onto the SiNWs array by bipolar magnetron sputtering [22]. The use of bipolar sputtering (Magpuls QP-1000/20 10 kW pulse unit) with two chromium targets (7.5 × 35 cm, 99.99% purity, from Neyco), instead of conventional DC sputtering is beneficial for well-crystallized nanostructures. The current was set at 5 A, with a duty cycle of 75% and a frequency of 1250 Hz. The deposition was achieved in Ar/N_2 gas mixture (150/120 sccm) at a pressure of 5 mTorr (0.66 Pa). Three deposition times were tested, namely 175, 210 and 350 s in order to obtain CrN nanostructures with different thicknesses. The deposition times correspond to equivalent thicknesses of 290, 550 and 900 nm, as measured on a flat silicon substrate set in the chamber, using a stylus profilometer.

2.4. Sample characterization

2.4.1. Structural and surface characterization

The top and cross section morphology of the SiNWs-CrN were investigated using scanning electron microscopy (SEM), (JEOL JSM 7500F microscope), while the crystallinity of the sample was examined by X-ray diffraction (PANalytical X'pert Pro, Cu Kα radiation λ= 0.1546 nm).

Structural investigation was carried out using a Tecnai T20 transmission electron microscope, working under 200 kV. The sample was deposited on a TEM grid for observation.

The surface chemistry of the samples was evaluated by X-ray photoelectron spectroscopy (Thermo Scientific K-Alpha, Al Kα radiation 1486.68 eV) with a spot size of 250×250 μm. The core level and survey spectra were acquired at 20 and 150 eV, respectively, with 20 and 3 scans. A flood gun was used for charge compensation. No additional binding energy shift (to C_{1s} signal) was required.

2.4.2. Electrochemical characterization

Electrochemical studies of SiNWs-CrN electrodes were conducted at room temperature in three-electrode electrochemical system. SiNWs-CrN sample, Ag/AgCl and Pt foil were used as working,

reference and counter electrodes, respectively. Only SiNWs-CrN active material was in contact with the electrolyte (S =0.5 cm^2). Silver paste was used to ensure good contact with the current collector. The electrodes were evaluated by Cyclic voltammetry (CV), Galvanostatic charge-discharge (GCD) and Electrochemical Impedance Spectroscopy (EIS) measurement in H_2SO_4 (0.5 M) aqueous solution.

The areal capacitance C, was calculated from the equation below [1]:

$$C = \frac{\Delta i}{2v} \quad (1)$$

$$C = \frac{I}{dV/dt} \quad (2)$$

Where:

C is the areal capacitance.

Δi is the average of the intensity difference between the upper and the lower part of the cyclic voltammetry curve.

v is the scan rate.

I is the applied current.

dV is the potential window and dt is the discharge time.

3. Results and discussion

The surface morphologies of the SiNWs and SiNWs-CrN electrodes are evaluated by SEM images as shown in Figure 1. Figure 1a displays the top view SEM image of SiNWs grown on a silicon wafer, revealing a high density of nanowires with an average diameter in the range of 30-80 nm.

(Figure 1b-d) reveals that the SiNWs are covered uniformly with small cubic CrN crystallites. It can be also noticed a continuous increase of the CrN film thickness on the SiNWs substrate upon increasing deposition time. Such results are expected to have an impact on the specific capacitance of SiNWs-CrN electrodes. As the deposition time increases, the SiNWs tend to stand up: more ends

of SiNWs are visible in top view. This effect can be attributed to stress generated during the deposition due to the misfit between CrN and Si nanowires [24].

In our case, the nanostructures are deposited on silicon substrates, which means that material quantity available is very low, and therefore, in contrast to powder, the Brunauer-Emmett-Teller (BET) analysis is not possible. The only possible way to estimate the surface area is from SEM images.

The formation of CrN crystallites is confirmed by XRD measurement (Figure 2). The pristine SiNWs exhibit three diffraction peaks which can be assigned to silicon and gold nanoparticles (used for the SiNWs growth). XRD patterns of the SiNWs-CrN electrodes with different CrN thicknesses show the presence of two broad peaks at 37.4° and 43.1°, with a decrease of Si (111) peak intensity. These two distinct peaks can be assigned to the (111) and (200) diffraction planes of cubic CrN [25, 26].

The surface chemistry compositions were investigated by XPS analyses (Figure 3). The surface of the as grown SiNWs consists of Si/SiO_2, are confirmed by Si 2p and O 1s core level spectra (Figure 3a-b). The high-resolution XPS spectrum of the Si 2p contains three contribution, centred at 99.3, 100.0 and 103.2eV attributed to Si $2p_{3/2}$, Si $2p_{1/2}$ and SiO_2, respectively [27]. The silicon oxide formation is also attested with a major peak at 532.6 eV (Figure 3b) [28]. These results are in good accordance with previous reported data [29]. Once the SiNWs are coated with CrN layers, the Si 2p signal vanishes while Cr 2p and N 1s signals appear, indicating a homogeneous coating of the analysed surface (Figure 3c-d). The high-resolution XPS spectrum of Cr 2p signal consists of two major peaks due to Cr $2p_{3/2}$ and Cr $2p_{1/2}$ spin orbit coupling. The Cr $2p_{3/2}$ level can be fitted with three peaks centred at 574.3, 575.3 and 576.6 eV assigned to CrN, Cr (O, N) and Cr_2O_3, respectively [30]. The surface oxidation of chromium is confirmed by a contribution at 531.0 eV on O 1s level. Such surface oxidation is expected, as no sample etching is done prior to the analysis. The formation of CrN is attested on the N 1s core level spectrum (Figure. 3c) with a major contribution at 396.4 eV in addition to oxy-nitride formation detected at 398.3 eV [30, 31].

The SiNWs-CrN substrate was further characterized by transmission electron microscopy (TEM) (Figure 4). TEM images showed a herringbone structure due to the deposition of CrN on SiNWs. This peculiar nanostructure, which contains highly nanoporous channels, is expected to contribute to the electrode capacitance enhancement. The electron diffraction (ED) pattern of a silicon nanowire coated with CrN (500 nm) confirms the crystallinity of the CrN layer on the SiNW. The ED pattern exhibits multiples rings around the central spot, characteristic to the polycrystalline nature of the CrN film. The indexation of these rings revealed the cubic structure of CrN film (Space group 225, $Fm\bar{3}m$). These results are in agreement with the XRD analyses.

Figure 5 display the CV curves of the SiNWs and SiNWs-CrN (550 nm) electrodes recorded at the same scan rate of 100 $mV.s^{-1}$ in 0.5 M H_2SO_4 electrolyte. By comparison, it is clear that SiNWs-CrN (550 nm) electrode has largest area with enhanced capacitive current compared to pristine SiNWs, indicating higher specific capacitance. The areal capacitance of SiNWs at 100 $mV.s^{-1}$ was measured to be 0.16 $mF.cm^{-2}$ versus 54 $mF.cm^{-2}$ for SiNWs-CrN (550nm) electrode.

(Figure 6a–c) depict the CV curves of SiNWs-CrN electrodes obtained at various scan rates in potential range of (0 - 0.8 V). The quasi-rectangular shapes of CV curves indicating that the SiNWs-CrN electrodes have obvious super-capacitive characteristic. However, at higher scan rates, CV curves become more distorted due to the increase of internal electrode resistivity.

GCD curves of SiNWs-CrN electrodes at a current density of 2 $mA.cm^{-2}$ are displayed in Figure 7. SiNWs-CrN 900 nm electrode displays the smallest IR drop of (0.12 V) followed by SiNWs-CrN 550 nm (0.13 V) and 290 nm (0.19 V),respectively. It can be also seen that the IR drop decreases with increasing the CrN thickness, indicating the good conductivity of CrN layers. This can be explained by the increase of the CrN coating density, as observed in SEM analysis.

In contrast, to the SiNWs electrode which exhibits a capacitance of 1.55 $mF.cm^{-2}$ under different scan rates, the areal capacitance values of the SiNWs-CrN electrodes, calculated from the CV curves (at a scan rate of 5 $mV.s^{-1}$) are as high as 80, 180 and 120 $mF.cm^{-2}$ for 290, 550 and 900 nm CrN coated

SiNWs, respectively. Furthermore, the areal capacitances was calculated from the GCD curves, and found to be 5.2, 31.8 and 16.8 $mF.cm^{-2}$ at a current density of 1.6 $mA.cm^{-2}$ for 290, 550 and 900 nm CrN coated SiNWs, respectively. Since the areal capacitance of SiNWs-CrN electrode reached 180 $mF.cm^{-2}$ while those of EDLC is limited to 1-100 $\mu F.cm^{-2}$. The charged storage mechanism of CrN coating is believed to be predominantly pseudo-capacitive.

The variation of the areal capacitance with scan rate and current density is displayed in (Figure 8). It is clear that the SiNWs-CrN 550 nm electrode has the highest capacitance value. Whereas the SiNWs-CrN 290 nm show the lowest capacitance. In order to investigate the relationship between the thickness of CrN and the performances of SiNWs-CrN electrodes, we have varied CrN thickness from 290 to 900 nm. It is seen that, the areal capacitance increase with the CrN thickness up to 550 nm, then is stabilized at 180 $mF.cm^{-2}$ as thickness reaches 550 nm. At higher thickness, the capacitance decreases. We should recall that the TEM analysis showed that SiNWs-CrN electrodes having a herringbone structure with highly nanoporous channels (Figure 4) which is expected to contribute to capacitance enhancement of the electrode. Further increase of CrN thickness (from 550 to 900 nm) would lead to capacitance decrease. The structural analysis by electron microscopy indicated that a continuous increase of the CrN film thickness on the SiNWs as observed by SEM images, suggesting that parts of the surface are inaccessible when the CrN thickness reaches 900 nm. This leads to insufficient ion transport and adsorption. Such behavior can be related to the amounts of CrN deposits and the surface area of different electrodes. Hence, both from a microstructural and an electrochemical characterization we can conclude that, around 550 nm is an optimal thickness to obtain a highest areal capacitance.

The comparison of areal capacitance of our electrodes with those of other nanostructures reported in literature are listed in Table 1. The areal capacitance of SiNWs-CrN 550 nm (130 and 31.8 $mF.cm^{-2}$ at 10 $mV.s^{-1}$ and 1.6 $mA.cm^{-2}$, respectively) is higher than of CrN thin film Ref [21] (in the range of 12.8 $mF.cm^{-2}$ at 1.0 mA cm^{-2}). Much higher than of MnO_2-SiNWs electrodes ref [33] and [12] (in

the range of 21.296 and 13.38 mF.cm^{-2} at 10 mV.s^{-1} respectively) and much higher than of carbon-SiNWs electrodes ref [11] (in the range of 25.6 mF.cm^{-2} at 0.1 mA cm^{-2}).These results confirm the high performance of SiNWs-CrN composites for ECs application. The superior performance of SiNWs-CrN 500 nm can be attributed to the larger surface area (highly nanoporous channels), which can provide good contact between electrolyte and active material, resulting in an improvement in areal capacitance. It is worth to mention that thinner film (290nm) may not have sufficient CrN active material, whereas thicker film (900 nm) may block the diffusion of electrolyte ion into electrode internal structure and pores.

EIS measurement (Figure 9) depicts the Nyquist plots of SiNWs-CrN electrodes. The charge transfer resistance (R_{ct}) is calculated to be about 146, 89 and 83 Ω for SiNWs-CrN 290, 550 and 900 nm electrodes. Indicating that the CrN layers can obviously reduce the charge transfer resistance and the electrodes can become more conductive as the thickness of the CrN layer increases.

The cycling stability of SiNWs-CrN 500 nm electrode at scan rate of 100 mV.s^{-1} is presented in Figure 10. As can be seen the electrode can sustain 92% of its initial capacitance value after 15000 cycles. Such cycling stability allows the use of these 3 D SiNWs@CrN electrodes for micro-supercapacitors.

4. Conclusion

In this work, we reported the synthesis of 3 D nanostructured electrodes made of chromium nitride (CrN) layer deposited on silicon nanowires (SiNWs) arrays using bipolar magnetron sputtering method. SEM and TEM analysis showed that the SiNWs are covered uniformly with CrN forming a twisted bundle-like nanostructure with high surface area. The results of electrochemical measurements showed that the SiNWs-CrN (550 nm) electrode has the highest areal capacitance of 180 mF.cm^{-2} at a scan rate of 5 mV.s^{-1} and 31.8 mF.cm^{-2} at high current density of 1.6 mA.cm^{-2} with 92% of its initial specific capacitance value after 15000 cycles in 0.5 M H_2SO_4 electrolyte. These results suggest that coating SiNWs with transition metal nitride such as CrN is a promising way for the construction of high-energy storage systems.

Acknowledgement

The Synthesis Irradiation and Analysis of Materials (SIAM), PC² and MORPH-IM platforms of UNamur are acknowledged for XPS, XRD and SEM measurements. JFC is Senior Research Associate at the F.R.S-FNRS. Financial support from the Centre National de la Recherche Scientifique (CNRS), the University of Lille, and the Hauts-de-France region is gratefully acknowledged. The silicon nanowires have been fabricated using equipments of the NanoRennes platform.

References

[1] A. Guerra, A. Achour, S. Vizireanu, , G. Dinescu, S. Messaci, T. Hadjersi, R. Boukherroub, J. J. Pireaux, ZnO/carbon nanowalls shell/core nanostructures as electrodes for supercapacitors. Appl. Surf. Sci. 481 (2019) 926–932.

[2] X. Zhou, B. Xu, Z. Lin, D. Shu, L. Ma, Hydrothermal synthesis of flower-like MoS2 nanospheres for electrochemical supercapacitors. J. Nanoscience. Nanotechnology, 14(9) (2014) 7250-7254.

[3] P. Simon, Y. Gogotsi, Materials for electrochemical capacitors, Nat. Mater. 7 (2008) 845–854.

[4] M. Mandal, D. Ghosh, S.S. Kalra, C. K. Das, High performance supercapacitor electrode material based on flower like MoS2/reduced graphene oxide nanocomposite. Int. J. Lat. Res. Sci. Technol, (2014) 3, 65.

[5] G.R. Li, Z.L. Wang, F.L. Zheng, Y.N. Ou, Y.X Tong, ZnO@MoO3 core/shell nanocables: facile electrochemical synthesis and enhanced supercapacitor performances, J. Mater. Chem. 21 (2011) 4217–4221.

[6]] P.M. Kulal, D.P. Dubal, C.D. Lokhande, V.J. Fulari, Chemical synthesis of Fe_2O_3 thin films for supercapacitor application, J. All. Comp, 509 (2011) 2567–2571.

[7] J. P. Alper, M. Vincent, C. Carraro, R. Maboudian, Silicon carbide coated silicon nanowires as robust electrode material for aqueous micro-supercapacitor. Appl. Phy. Lett, 100.16 (2012) 163901.

[8] F. Thissandier, N. Pauc, T. Brousse, P. Gentile, S. Sadki, Micro-ultracapacitors with highly doped silicon nanowires electrodes. Nanoscale Res. Lett, 8.1 (2013) 38.

[9] N. Berton, M. Brachet, F. Thissandier, J. Le Bideau, P. Gentile, G. Bidan, S. Sadki, Wide-voltage-window silicon nanowire electrodes for micro-supercapacitors via electrochemical surface oxidation in ionic liquid electrolyte. Electroch. Comm, 41 (2014) 31-34.

[10] F. Thissandier, P. Gentile, N. Pauc, T. Brousse, G. Bidan, S. Sadki, Tuning silicon nanowires doping level and morphology for highly efficient micro-supercapacitors. Nano. Energy, 5 (2014) 20-27.

[11] R.R. Devarapalli, S. Szunerits, Y. Coffinier, M.V. Shelke, R. Boukherroub, Glucose-derived porous carbon-coated silicon nanowires as efficient electrodes for aqueous micro-supercapacitors. ACS. Appl. Mater. Inter, 8.7 (2016) 4298-4302.

[12] D. P. Dubal, D. Aradilla, G.Bidan, P. Gentile, T. J. Schubert, J. Wimberg, P. Gomez-Romero, 3D hierarchical assembly of ultrathin MnO2 nanoflakes on silicon nanowires for high performance micro-supercapacitors in Li-doped ionic liquid. Sci. Rep, 5 (2015) 9771.

[13] A. Achour, M. Islam, I. Ahmad, L. Le Brizoual, A. Djouadi, T. Brousse, Influence of surface chemistry and point defects in TiN based electrodes on electrochemical capacitive storage activity, Scrip. Mater, 153 (2018) 59-62.

[14] P. Yang, D. Chao, C. Zhu, X. Xia, Y. Zhang, X. Wang, H.J. Fan, Ultrafast-charging supercapacitors based on corn-like titanium nitride nanostructures. Adv. Sci, 3.6 (2016) 1500299.

[15] E. Kao, C. Yang, R. Warren, A. Kozinda, L. Lin, ALD titanium nitride on vertically aligned carbon nanotube forests for electrochemical supercapacitors. Sensors. Actuators. A: Physical, 240 (2016) 160-166.

[16] N. Ouldhamadouche, A. Achour, R. Lucio-Porto, M. Islam, S. Solaymani, A. Arman, A. Ahmadpourian, H. Achour, L. Le Brizoual, M. A. Djouadi, T. Brousse, Electrodes based on nano-

tree-like vanadium nitride and carbon nanotubes for micro-supercapacitors, J. Mater. Sci. Tech 34 (2018) 976-982.

[17] A. Achour, R. Lucio-Porto, S. Solaymani, M. Islam, I. Ahmad, T. Brousse, Reactive sputtering of vanadium nitride thin films as pseudo-capacitor electrodes for high areal capacitance and cyclic stability, J. Mater. Sci.: Mater. Electron, 29 (2018) 13125-13131

[18] X. Lu, M. Yu, T. Zhai, G. Wang, S. Xie, T. Liu, Y. Li, High energy density asymmetric quasi-solid-state supercapacitor based on porous vanadium nitride nanowire anode. Nano. Lett, 13.6 (2013) 2628-2633.

[19] A. Djire, J.B. Siegel, O. Ajenifujah, L. He, L.T. Thompson, Pseudocapacitive storage via micropores in high-surface area molybdenum nitrides. Nano. Energy, 51 (2018) 122-127.

[20] M. Arif, A. Sanger, A. Singh, Sputter deposited chromium nitride thin electrodes for supercapacitor applications. Mater. Lett, 220 (2018) 213-217.

[21] B. Wei, H. Liang, Zhang, D., Z. Wu, Z. Qi, Z. Wang, CrN thin films prepared by reactive DC magnetron sputtering for symmetric supercapacitors. J. Mater. Chem. A, 5.6 (2017) 2844-2851.

[22] E. Haye, J. L. Colaux, P. Moskovkin, J. J. Pireaux, S. Lucas, Wide range investigation of duty cycle and frequency effects on bipolar magnetron sputtering of chromium nitride. Surf. Coat. Tech, 350(2018) 84-94.

[23] N. Verplanck, E. Galopin, J. C. Camart, V. Thomy, Y. Coffinier, R. Boukherroub, Reversible Electrowetting on Superhydrophobic Silicon Nanowires. Nano. Lett, 7 (2007) 813-817.

[24] M. Muraoka, N. Settsu, M. Saka, Residual-strain-induced nanocoils of metallic nanowires. J. Nanosci. Nanotechnology, 8 (2008) 439-442.

[25] P. Hones, R. Sanjines, F. Lévy, Characterization of sputter-deposited chromium nitride thin films for hard coatings. Surface and Coatings Technology, 94(1997) 398-402.

[26] E.Haye, J. L. Colaux, P. Moskovkin, J. J. Pireaux, S. Lucas, Wide range investigation of duty cycle and frequency effects on bipolar magnetron sputtering of chromium nitride. Surface and Coatings Technology, 350 (2018) 84-94.

[27] M.A. Gharavi, S. Kerdsongpanya, S. Schmidt, F. Eriksson, N.V. Nong, J. Lu, B. Balke, D. Fournier, L. Belliard, A. le Febvrier, C. Pallier, P. Eklund, Microstructure and thermoelectric properties of CrN and CrN/Cr2N thin films, J. Phys D: Appl. Phys, 51 (2018) 355302.

[28] D.S. Jensen, S.S. Kanyal, N. Madaan, M.A. Vail, A.E. Dadson, M.H. Engelhard, M.R. Linford, Silicon (100)/SiO_2 by XPS, Surf Sci. Spectra 20 (2013) 36–42.

[29] I. Kurylo, M. Dupré, S. Cantel, C. Enjalbal, H. Drobecq, S. Szunerits, O. Melnyk, R. Boukherroub, Y. Coffinier, Characterization of peptide attachment on silicon nanowires by X-ray photoelectron spectroscopy and mass spectrometry, Analyst 142 (2017) 969–978.

[30] I. Milošev, H.H. Strehblow, B. Navinšek, Comparison of TiN, ZrN and CrN hard nitride coatings: Electrochemical and thermal oxidation, Thin Solid Films 303 (1997) 246–254.

[31] H.C. Barshilia, N. Selvakumar, B. Deepthi, K.S. Rajam, A comparative study of reactive direct current magnetron sputtered CrAlN and CrN coatings, Surf. Coat. Technol. 201 (2006) 2193–2201.

[32] P. Zaumseil, High-resolution characterization of the forbidden Si 200 and Si 222 reflections, J. Appl. Cryst, 48 (2015) 528–532.

[33] F. Moulai, T. Hadjersi, M. Ifires, A. Khen, N. Rachedi, Enhancement of Electrochemical Capacitance of Silicon Nanowires Arrays (SiNWs) by Modification with Manganese Dioxide MnO 2. Silicon, (2019) 1-12

Table Captions

Table 1. Performance of SiNWs-CrN electrode.

Figure Captions

Figure 1. Top view SEM images of (a) raw SiNWs, (b) SiNWs-CrN 290 nm, (c) SiNWs-CrN 550 nm and (d) SiNWs-CrN 900 nm.

Figure 2. XRD pattern of SiNWs coated with CrN thin layers. The (*) corresponds to forbidden Si reflection, due to multiple diffraction in the Si substrate [32].

Figure 3. XPS analysis of SiNWs-CrN electrode materials: High resolution XPS spectra of (a) Si 2p, (b) O 1s, (c) N 1s and (d) Cr 2p core levels.

Figure 4 Transmission electron microscopy (TEM) images (a) to (c) and electron diffraction (d) of SiNWs-CrN (500nm).

Figure 5: CV curves of SiNWs and SiNWs-CrN (550 nm) electrodes recorded in 0.5 M H_2SO_4 at a scan rate of 100 $mV \cdot s^{-1}$. Inset CV SiNWs.

Figure 6: CV curves recorded in 0.5 M H_2SO_4 at various scan rates. (a) SiNWs-CrN 290 nm, (b) SiNWs-CrN 550 nm, (c) SiNWs-CrN 900 nm.

Figure 7: Charge-discharge curves of SiNWs-CrN electrodes with different CrN thiknesses recorded at 2 $mA.cm^{-2}$.

Figure 8: Variation of areal capacitance of SiNWs-CrN at different (a) scan rates and (b) current densities.

Figure 9: Nyquist impedance plots for CrN-SiNWs (290, 550 and 900 nm) electrodes.

Figure 10: Evolution of the capacitance for CrN-SiNWs 550 nm electrode after 15,000 consecutive cycles at scan rate of 100 $mV.s^{-1}$.

Table 1

Film deposition	Capacitance ($mF.cm^{-2}$)	references
CrN-SiNWs	131 (10 $mv.s^{-1}$) 31.8 (1.6 $mA.cm^{-2}$)	This work
CrN thin film	12.8 (1.0 $mA.cm^{-2}$)	[21]
MnO_2-SiNWs	21.296 (10 $mv.s^{-1}$)	[33]
MnO_2-SiNWs	13.38 (10 $mv.s^{-1}$)	[12]
Carbon-SiNWs	25.6 (0.1 mA cm^{-2})	[11]

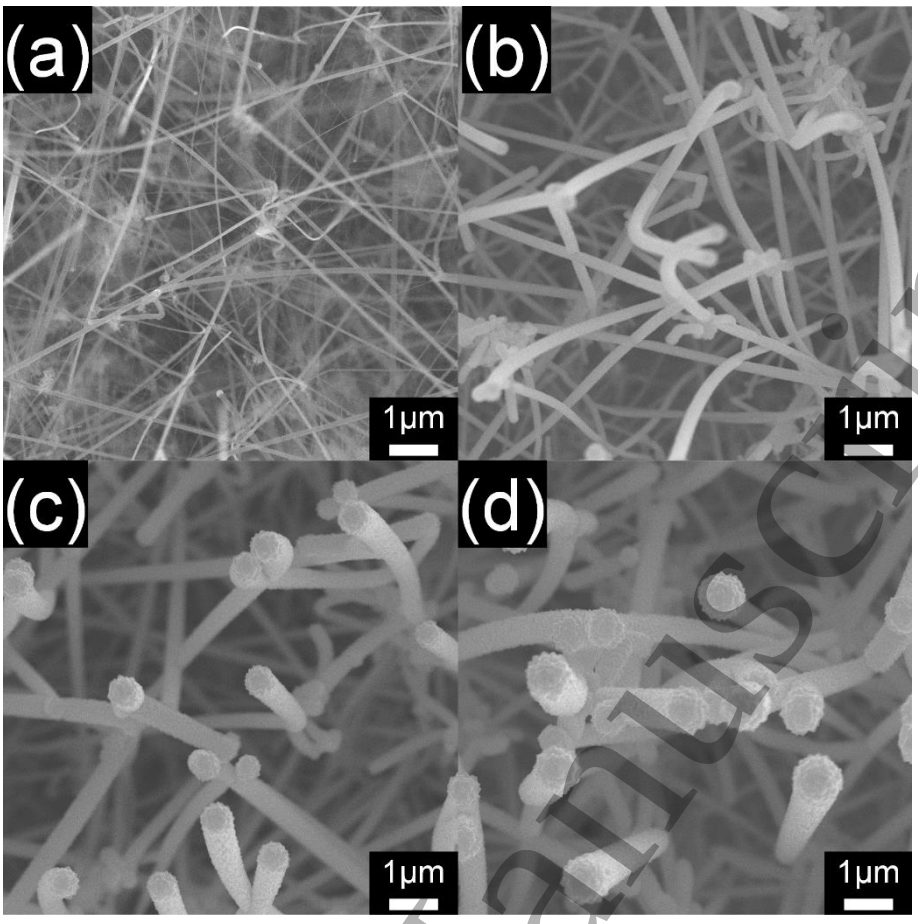

Figure 1

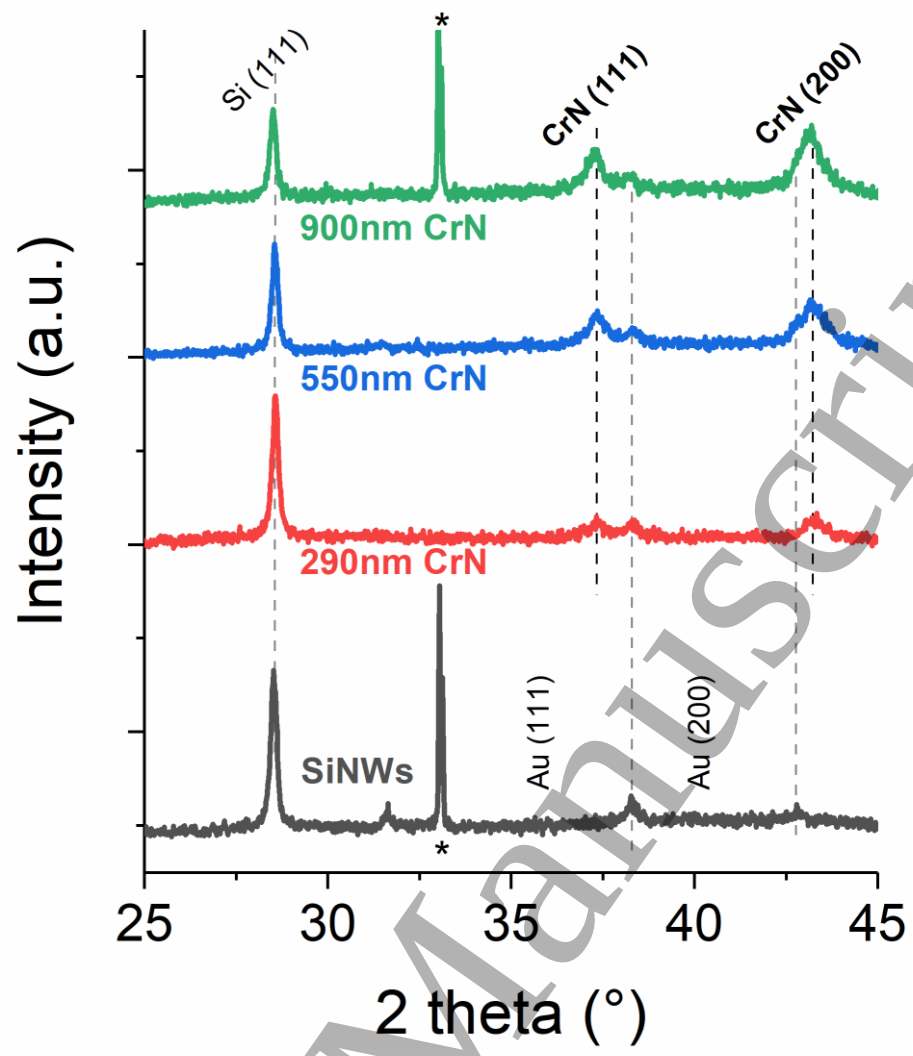

Figure 2

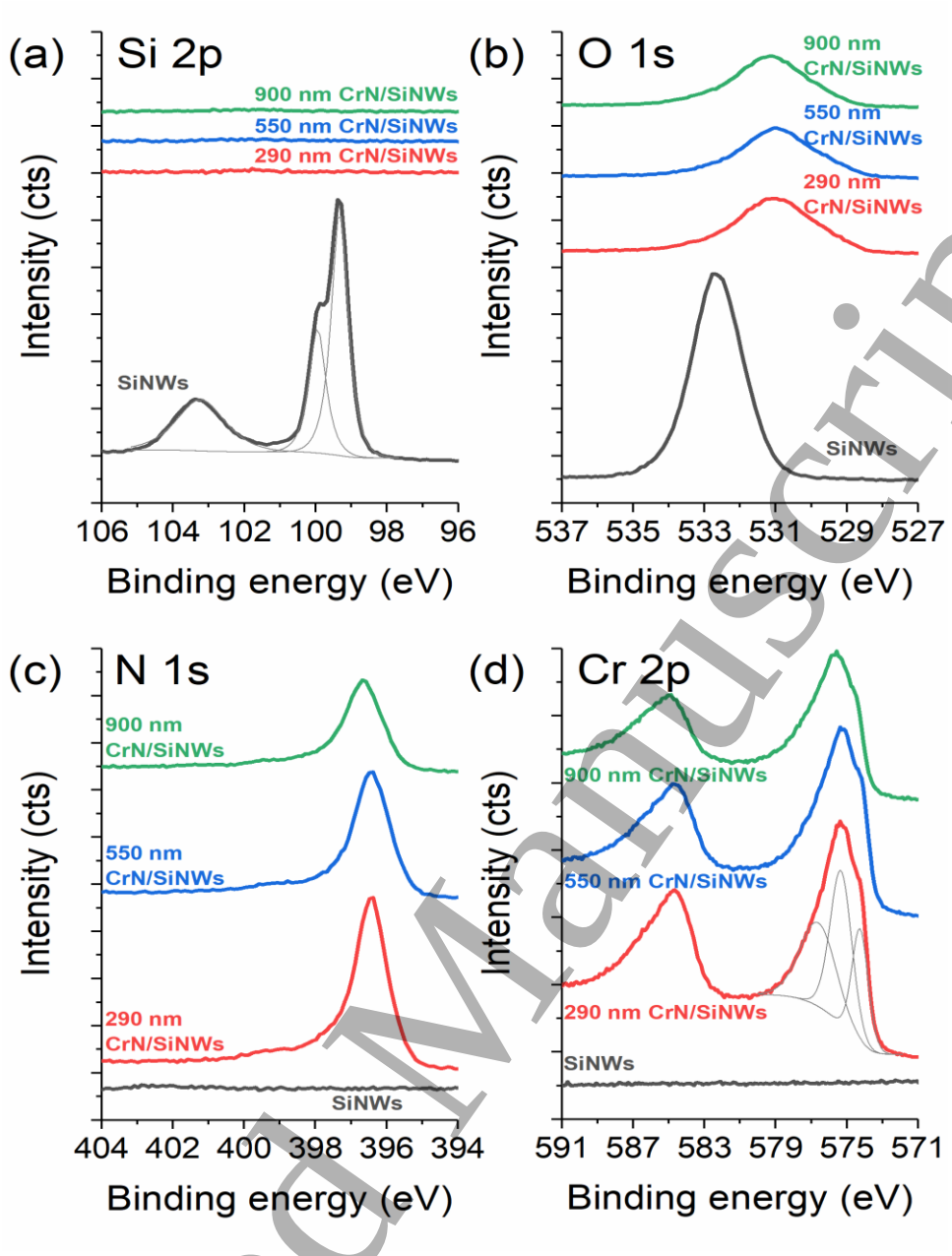

Figure 3

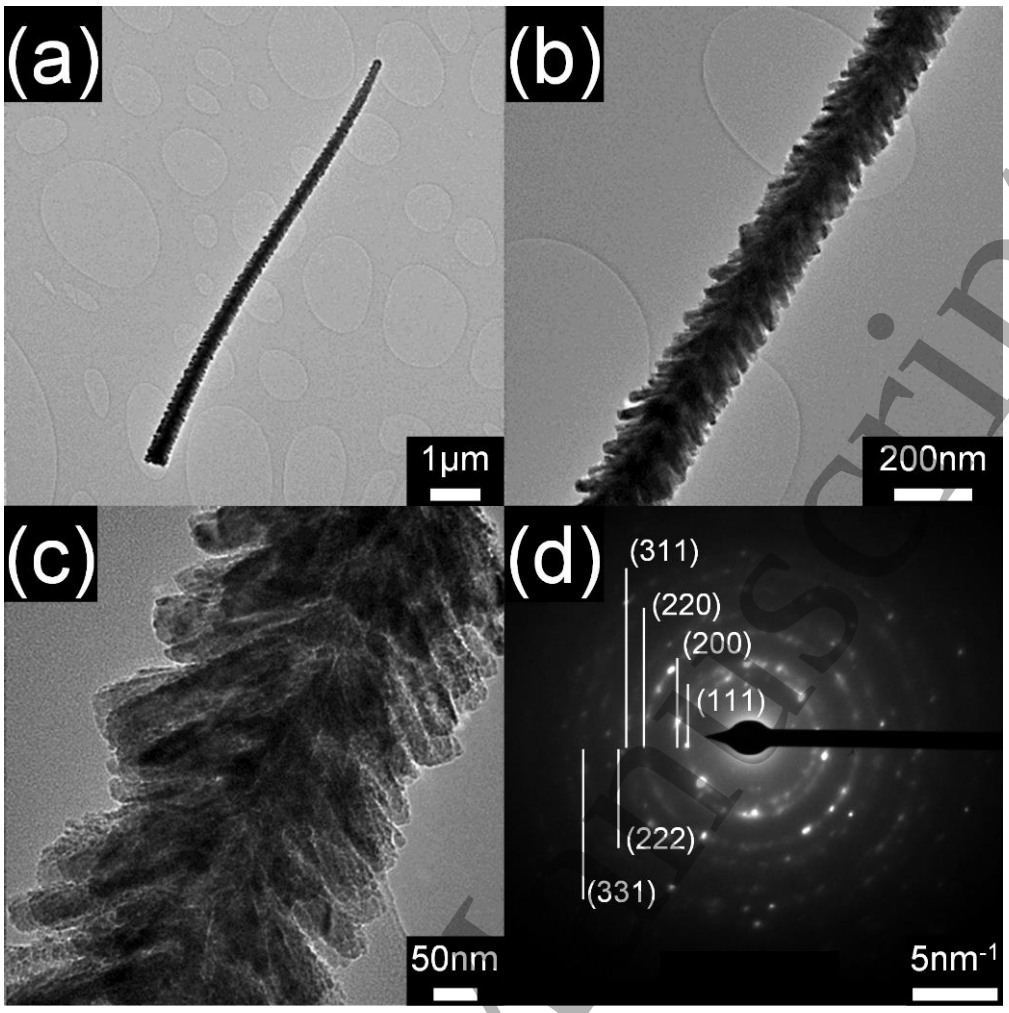

Figure 4

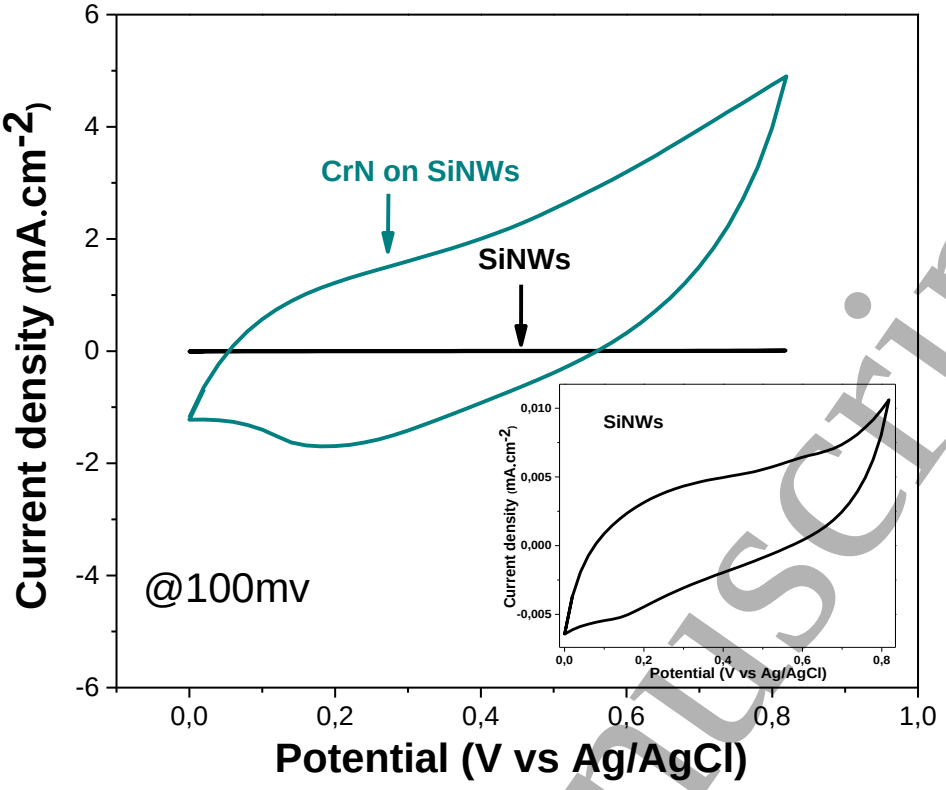

Figure 5

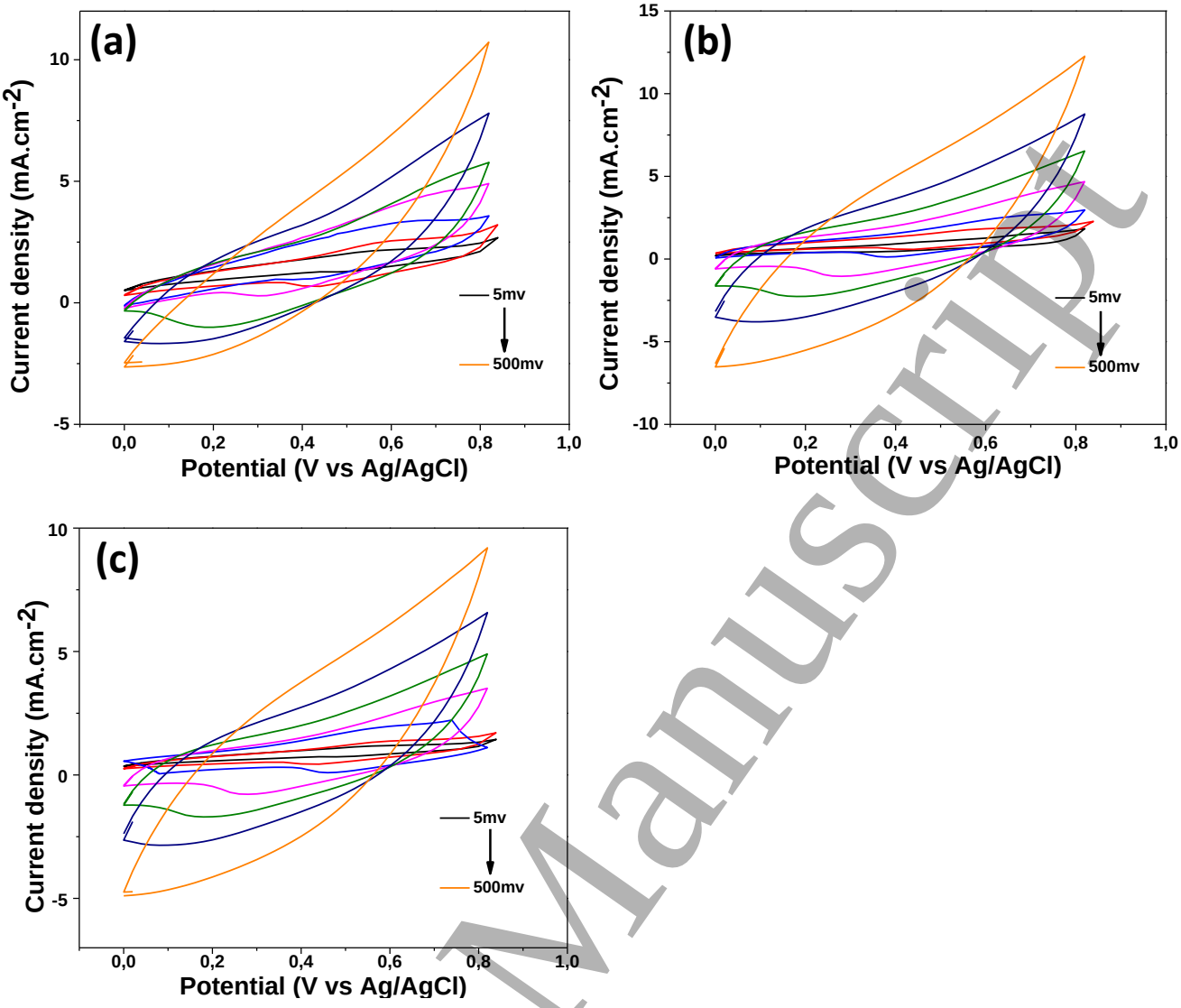

Figure 6

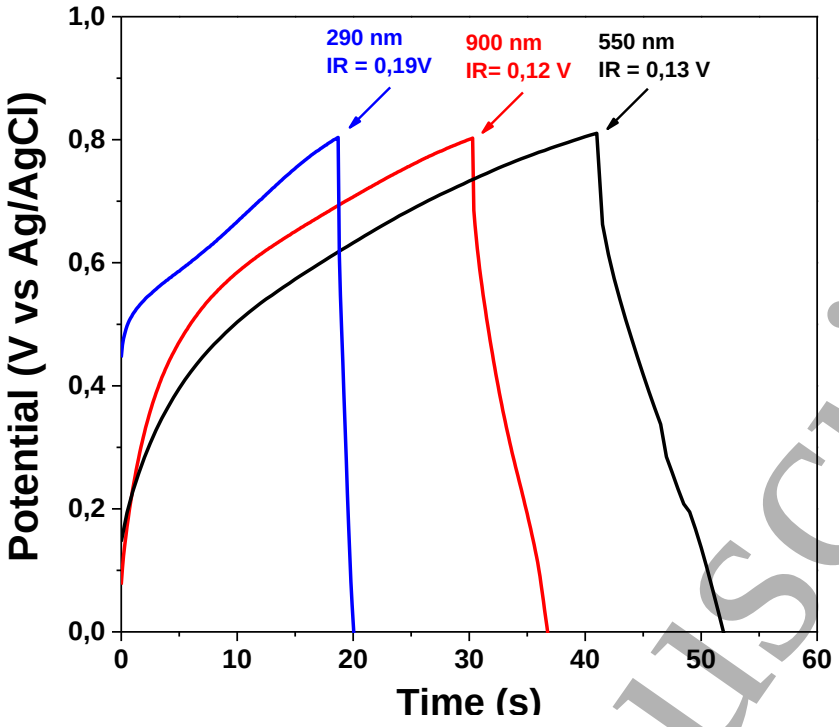

Figure 7

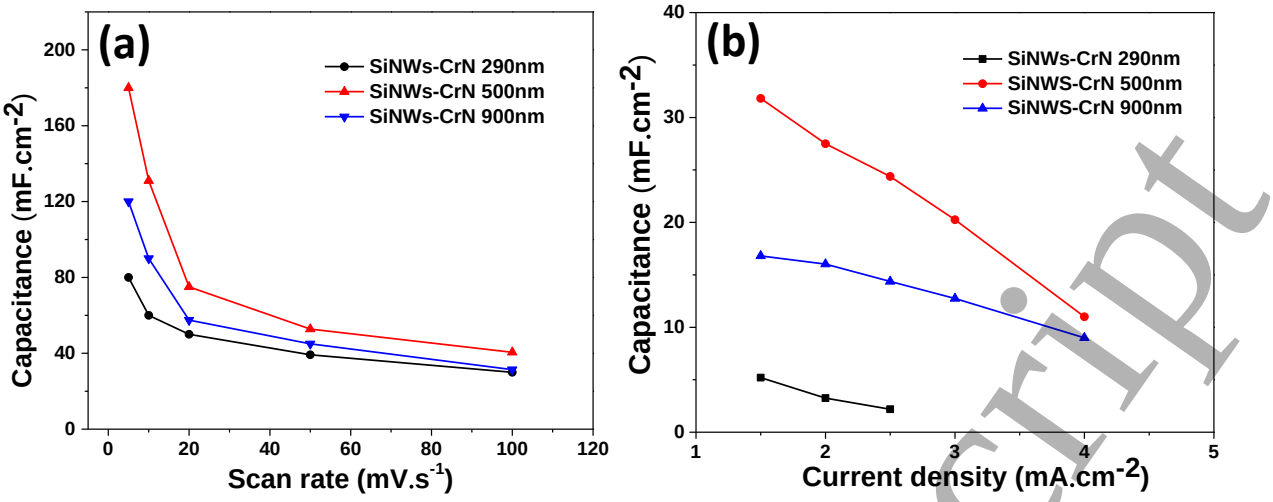

Figure 8

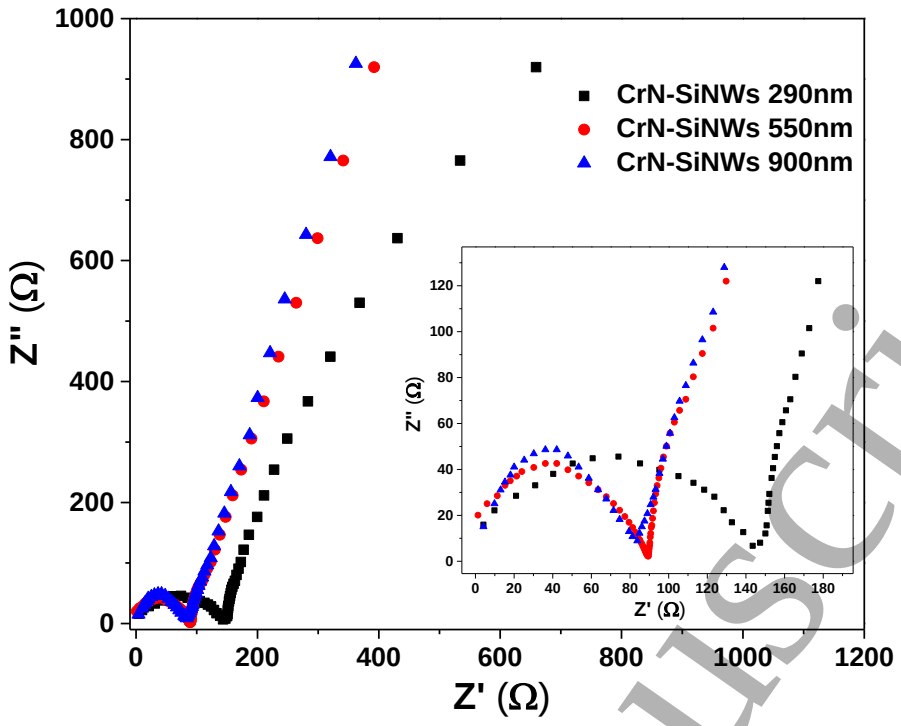

Figure 9

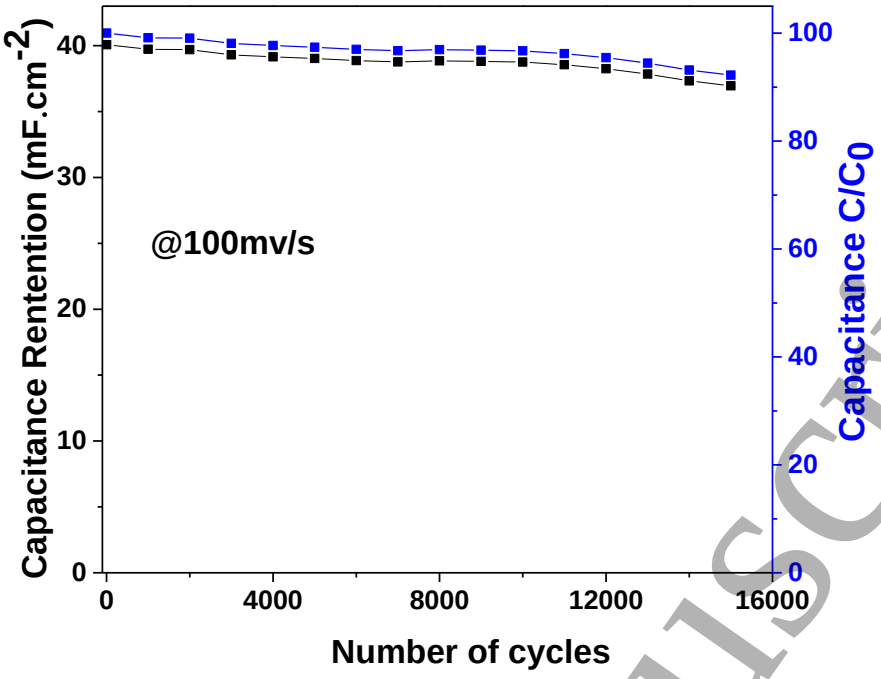

Figure 10